A Numerical Study of the Vibration Spectrum for a Double-Walled Carbon Nanotube Model

Marianna A. Shubov[1]*and Matthew P. Coleman[2]
[1]*Department of Mathematics & Statistics, University of New Hampshire, Durham*
[2]*Department of Mathematics and Computer Science, Fairfield University, Fairfield*
USA

1. Introduction

In this paper we offer a series of new results devoted to the numerical analysis of a double-walled carbon nanotube model. This model is given in the form of two coupled Timoshenko beams connected through the distributed Van der Waals force (Gibson et al., 2007; Ru, 2000). Typically, nanotubes can be modeled as quantum systems and studied by a molecular simulations approach, or as classical systems (such as flexible beams, shells membranes (Mahan, 2002; Pantano et al., 2003; 2004; Wang et al., 2004; 2005)), or as specific hybrid models (Wang, 2005). The choice of model in any situation involves a tradeoff in that, while molecular models may yield more accurate results, implementing them is extremely time and labor intensive, which is not the case for models from continuum mechanics.

The scientific and engineering communities have acknowledged the very desirable properties of carbon nanotubes (CNTs) and their potential use in wide-ranging applications. The author of (Jamieson, 2000) argues that nanotechnology, mainly due to CNTs, may impact technology more than did the silicon revolution. Depending on the atomic structure, CNTs have electrical properties that can range from those of metals to those of semiconductors. The mechanical properties of CNTs are also unique. They possess exceptionally high specific stiffness and specific strength; they are extremely elastic, being able to bend through a complete 360° without noticeable damage. The application potential for materials with these properties is almost limitless.

Developing mathematical models for CNTs is of critical importance. Such models must be verified and quantified by performing and analyzing experiments. As we have mentioned, two groups of models exist: molecular simulation models and continuum mechanics models. Continuum models are generally based on traditional engineering models such as beams, shells, or membranes. The nanotubes are treated as continuous materials with definite geometries and common material properties such as *Young's modulus*. In contrast, molecular models consider each atom, and mathematically define the interactions among the atoms. Based on their work on atomic simulations of CNTs, the authors of (Jakobson et al., 1996) provide a justification for incorporating continuum mechanics models into CNTs study,

*Corresponding author: Marianna A. Shubov, Department of Mathematics & Statistics, University of New Hampshire, Durham

stating that “The laws of continuum mechanics are amazingly robust and allow one to treat even intrinsically discrete objects only a few atoms in diameter.”

The most commonly used models are the following: the Euler–Bernoulli beam model, Timoshenko beam model, and flexible shell and membrane models. Typically, many models for multi-walled nanotubes allow for independent wall movement, and the wall interaction is a function of the local wall separation distance.

Vibration of a double-walled carbon nanotube (DWCNT) generated by a nonlinear interlayer Van der Waals force is studied in (Xu et al., 2006). The results indicate that the nonlinear factors of the Van der Waals force, on the one hand, have little effect on the coaxial free vibrations. On the other hand, these nonlinear factors greatly affect noncoaxial free vibrations. As is indicated in (Qian et al., 2002), although carbon nanotubes can have diameters only several times larger than the length between carbon atoms, continuum models have been found to describe their mechanical behavior very accurately, in many circumstances.

Our analysis of an initial boundary-value problem models small transversal vibrations of a double-walled carbon nanotube. The system of equations is similar to the ones mentioned in a number of papers (see references (Gibson et al., 2007; Jakobson et al., 1996; Pantano et al., 2003; Qian et al., 2002; Ru, 2001; Wang et al., 2006; Xu et al., 2006; Yoon et al., 2003)). The physical system consists of two nested nanotubes interacting through the distributed Van der Waals force; each nanotube is modeled as a Timoshenko beam with specific parameters. As pointed out in (Wang et al., 2006), “Unlike the Euler–Bernoulli beam model, the Timoshenko beam model allows for the effects of transverse shear deformation and rotary inertia. These effects become significant for carbon nanotubes with small length-to-diameter ratios that are normally encountered in applications.”

The model is given in the form of two coupled Timoshenko beams (i.e., in the form of four coupled hyperbolic partial differential equations). The system is equipped with a set of nonself-adjoint boundary conditions involving four independent complex parameters. Indeed, all other articles treating the Timoshenko model consider only the traditional energy-conserving boundary conditions, thus our treatment is a generalization of their work (as these latter conditions are just limiting special cases of the nonself-adjoint conditions treated herein). An asymptotic analysis of the eigenspectrum for this problem was performed in (Shubov & Rojas-Arenaza, 2010a;b;c), under certain simplifying assumptions. We must mention that the assumptions are somewhat restrictive—indeed, they cannot be satisfied by a physical double-walled carbon nanotube system. However, even for this simplified case, the necessary computations were extremely complex and cumbersome, and it is unclear if the more general problem even is tractable.

Regardless, this special case is a valid and interesting mathematical problem whose behavior should be quite similar to the more general physical problem. Thus, we feel that a study of the vibration spectrum for this case certainly will shed light on the spectrum of the more general problem, particularly by our choosing values for the physical parameters that are similar to those for physical carbon nanotubes.

The paper is organized as follows. In Section 2, we introduce the general mathematical model, perform separation of variables and rewrite the special case of the model treated in (Shubov & Rojas-Arenaza, 2010a) in dimensionless form. In Section 3, we present the asymptotic results derived in (Shubov & Rojas-Arenaza, 2010a). The Legendre-tau spectral method is described in Section 4, and in Section 5 we present our numerical results and comparison with the asymptotic results predicted by (Shubov & Rojas-Arenaza, 2010a).

2. The mathematical model

We consider the system consisting of two Timoshenko beams coupled through the van der Waals force, as given in (Shubov & Rojas-Arenaza, 2010a;b;c):

$$\sigma A_1 W_{1tt}(x,t) + k_1 G A_1[\Phi_{1x}(x,t) - W_{1xx}(x,t)] = -C[W_2(x,t) - W_1(x,t)] \tag{1}$$

$$\sigma I_1 \Phi_{1tt}(x,t) - E I_1 \Phi_{1xx}(x,t) + k_1 G A_1[\Phi_1(x,t) - W_{1x}(x,t)] = 0 \tag{2}$$

$$\sigma A_2 W_{2tt}(x,t) + k_2 G A_2[\Phi_{2x}(x,t) - W_{2xx}(x,t)] = C[W_2(x,t) - W_1(x,t)] \tag{3}$$

$$\sigma I_2 \Phi_{2tt}(x,t) - E I_2 \Phi_{2xx}(x,t) + k_2 G A_2[\Phi_2(x,t) - W_{2x}(x,t)] = 0. \tag{4}$$

For boundary conditions, the left end of each beam is free, while the right end of each is subject to the standard set of two-parameter boundary conditions:

$$W_{1x}(0,t) - \Phi_1(0,t) = \Phi_{1x}(0,t) = 0 \tag{5,6}$$

$$W_{2x}(0,t) - \Phi_2(0,t) = \Phi_{2x}(0,t) = 0 \tag{7,8}$$

$$k_1 G A_1[\Phi_1(L,t) - W_{1x}(L,t)] = \sigma I_1 \alpha_1 W_{1t}(L,t) \tag{9}$$

$$E\Phi_{1x}(L,t) = -\sigma \beta_1 \Phi_{1t}(L,t) \tag{10}$$

$$k_2 G A_2[\Phi_2(L,t) - W_{2x}(L,t) = \sigma I_2 \alpha_2 W_{2t}(L,t) \tag{11}$$

$$E\Phi_{2x}(L,t) = -\sigma \beta_2 \Phi_{2t}(L,t). \tag{12}$$

Here, $0 \leq x \leq L$ where L is the length of each beam, and $t \geq 0$. $W_i(x,t)$ is the transverse displacement of beam i, $\Phi_i(x,t)$ is the bending angle of beam i, $i = 1,2$. The physical and geometrical constants are as follows: σ is the mass per unit volume; E, Young's modulus; G, the shear modulus; A_i, the uniform cross-sectional area of beam i; I_i the uniform area moment of inertia of beam i; and k_i; the shear connection factor for beam i. We note that $E = 2(1+\nu)G$, where ν is the Poisson's ratio.
Further, we note the following:

$$\alpha_i = \beta_i = 0 \Rightarrow \text{ right end of beam } i \text{ is free} \tag{13}$$

$$\alpha_i = \beta_i = \infty \Rightarrow \text{right end of beam } i \text{ is clamped} \tag{14}$$

$$\alpha_i = \infty, \beta_i = 0 \Rightarrow \text{right end of beam } i \text{ is simply-supported} \tag{15}$$

$$\alpha_i = 0, \beta_i = \infty \Rightarrow \text{right end of beam } i \text{ is roller-supported.} \tag{16}$$

We separate variables by letting

$$W_j(x,t) = e^{-i\omega t} w_j(x),$$
$$\Phi_j(x,t) = e^{-i\omega t} \phi_j(x),$$

$j = 1, 2$, and, following the notation in (Shubov & Rojas-Arenaza, 2010a), the system (1)–(12) becomes

$$\omega^2 w_1(x) = \widehat{k}_1[\phi_1'(x) - w_1''(x)] + C_1[w_2(x) - w_1(x)] \tag{17}$$

$$\omega^2 \phi_1(x) = -\frac{E}{\sigma}\phi_1''(x) + \tilde{k}_1[\phi_1(x) - w_1'(x)] \tag{18}$$

$$\omega^2 w_2(x) = \widehat{k}_2[\phi_2'(x) - w_2''(x)] - C_2[w_2(x) - w_1(x)] \tag{19}$$

$$\omega^2 \phi_2(x) = -\frac{E}{\sigma}\phi_2''(x) + \tilde{k}_2[\phi_2(x) - w_2'(x)] \tag{20}$$

$$w_1'(0) - \phi_1(0) = 0 \tag{21}$$

$$\phi_1'(0) = 0 \tag{22}$$

$$w_2'(0) - \phi_2(0) = 0 \tag{23}$$

$$\phi_2(0) = 0 \tag{24}$$

$$\tilde{k}_1[\phi_1(L) - w_1'(L)] = -i\omega\alpha_1 w_1(L) \tag{25}$$

$$\frac{E}{\sigma}\phi_1'(L) = i\omega\beta_1\phi_2(L) \tag{26}$$

$$\tilde{k}_2[\phi_2(L) - w_2'(L)] = -i\omega\alpha_2 w_2(L) \tag{27}$$

$$\frac{E}{\sigma}\phi_2'(L) = i\omega\beta_2\phi_2(L). \tag{28}$$

Here, we have

$$\tilde{k}_i = \frac{k_i G A_i}{\sigma I_i}, \quad \widehat{k}_i = \frac{k_i G}{\sigma}, \quad C_i = \frac{C}{\sigma A_i}, \qquad i = 1, 2.$$

Again, following (Shubov & Rojas-Arenaza, 2010a), we consider the special case

$$\tilde{k}_1 = \tilde{k}_2 = \tilde{k}, \quad \widehat{k}_1 = \widehat{k}_2 = \widehat{k}. \tag{29}$$

We must note that these conditions cannot hold for a physical double-walled carbon nanotube (e.g., the shape factors must be different, $k_1 \neq k_2$). However, without these assumptions, the asymptotic treatment of the problem becomes extremely difficult, and possibly intractable. Thus, at this point in time, this particular special case is the only one for which there are analytical results with which to compare. We now cast the problem in dimensionless form. Following (Traill-Nash & Collar, 1953) and, more appropriately, (Coleman & Schaffer, 2010), we introduce dimensionless quantities as follows:

$$\begin{aligned}
&\widehat{x} = \frac{x}{L}, \quad \widehat{w}_i(\widehat{x}) = \frac{1}{L}w_i(x), \quad \widehat{\phi}_i(\widehat{x}) = \phi_i(x), \qquad i = 1, 2, \\
&\lambda = \sqrt{\frac{\sigma\tilde{k}}{E\widehat{k}}}L^2\omega, \quad \gamma_1 = \frac{\widehat{k}}{\tilde{k}L^2}, \quad \gamma_2 = \frac{E}{\sigma\tilde{k}L^2}, \\
&\alpha_i' = \frac{1}{\sigma A\tilde{k}L}\sqrt{\frac{E\widehat{k}}{\sigma\tilde{k}}}\,\alpha_i, \quad \beta_i' = \frac{1}{\sigma A\tilde{k}L^3}\sqrt{\frac{E\widehat{k}}{\sigma\tilde{k}}}\,\beta_i, \qquad i = 1, 2, \\
&C_i' = \frac{L^2}{\widehat{k}}C_i = \frac{L^2}{k_i G A_i}C, \qquad i = 1, 2.
\end{aligned} \tag{30}$$

We abuse notation, and use x, w_i, ϕ_i instead of $\widehat{x}, \widehat{w}_i$ and $\widehat{\phi}_i$, and the resulting dimensionless system is

$$-\gamma_2\lambda^2 w_1(x) = -\phi_1'(x) + w_1''(x) - C_1'[w_2(x) - w_1(x)] \tag{31}$$
$$-\gamma_1\gamma_2\lambda^2\phi_1(x) = \gamma_2\phi_1''(x) - \phi_1(x) + w_1'(x) \tag{32}$$
$$-\gamma_2\lambda^2 w_2(x) = -\phi_1'(x) + w_2''(x) + C_2'[w_2(x) - w_1(x)] \tag{33}$$
$$-\gamma_1\gamma_2\lambda^2\phi_2(x) = \gamma_2\phi_2''(x) - \phi_2(x) + w_2'(x), \qquad 0 < x < 1, \tag{34}$$
$$w_1'(0) - \phi_1(0) = 0 \tag{35}$$
$$\phi_1'(0) = 0 \tag{36}$$
$$w_2'(0) - \phi_2(0) = 0 \tag{37}$$
$$\phi_2'(0) = 0 \tag{38}$$
$$\phi_1(1) - w_1'(1) + i\alpha_1'\lambda w_1(1) = 0 \tag{39}$$
$$\gamma_2\phi_1'(1) - i\beta_1'\lambda\phi(1) = 0 \tag{40}$$
$$\phi_2(1) - w_2'(1) + i\alpha_2'\lambda w_2(1) = 0 \tag{41}$$
$$\gamma_2\phi_2'(1) + i\beta_2'\lambda\phi(1) = 0. \tag{42}$$

3. Asymptotic estimation of vibration spectrum

The first-order asymptotic estimation of the vibration frequencies for problem (31)–(42) is given in Theorem 2.5, of (Shubov & Rojas-Arenaza, 2010a); we present the results here, but in dimensionless form.

Theorem (Shubov, Rojas-Arenaza). *Assume that the boundary parameters α_i' and β_i', $i \geq 1, 2$, satisfy the following conditions*

$$\alpha_1' \neq \alpha_2', \quad \beta_1' \neq \beta_2', \quad \alpha_i' \neq \sqrt{\gamma_2}, \quad \beta_i' \neq \sqrt{\gamma_1}\,\gamma_2, \quad \textit{and}$$
$$\left|\frac{\alpha_i' - \sqrt{\gamma_2}}{\alpha_i' + \sqrt{\gamma_2}}\right| \neq \left|\frac{\beta_i' - \sqrt{\gamma_1}\,\gamma_2}{\beta_i' + \sqrt{\gamma_1}\,\gamma_2}\right|.$$

Then, the set of frequencies $-i\lambda$ of system (31)–(42) *splits into the following four separate branches:*

$$-i\lambda_n^{(1)} = \frac{1}{2\sqrt{\gamma_2}}\left[\log\frac{1-\alpha_1''}{1+\alpha_1''} + 2n\pi i\right] + O\left(\frac{1}{n}\right), \tag{43}$$
$$-i\lambda_n^{(2)} = \frac{1}{2\sqrt{\gamma_1}}\left[\log\frac{1-\beta_1''}{1+\beta_1''} + 2n\pi i\right] + O\left(\frac{1}{n}\right), \tag{44}$$
$$-i\lambda_n^{(3)} = \frac{1}{2\sqrt{\gamma_2}}\left[\log\frac{1-\alpha_2''}{1+\alpha_2''} + 2n\pi i\right] + O\left(\frac{1}{n}\right), \tag{45}$$
$$-i\lambda_n^{(4)} = \frac{1}{2\sqrt{\gamma_1}}\left[\log\frac{1-\beta_2''}{1+\beta_2''} + 2n\pi i\right] + O\left(\frac{1}{n}\right), \qquad n = \pm 1, 2, 3, \ldots \tag{46}$$

where

$$\alpha_i'' = \frac{1}{\sqrt{\gamma_2}}\alpha_i', \quad \beta_i'' = \frac{1}{\sqrt{\gamma_1}\,\gamma_2}\beta_i', \qquad i = 1, 2. \qquad \square$$

We note that log represents the complex logarithm, $\log z = \ln|z| + i \arg z$. We note also the important fact that the Van der Waals force between the two tubes does not appear in the first-order approximation.

4. The legendre-tau spectral method

We compare the asymptotic results of the Theorem with a numerical approximation of the spectrum using the Legendre-tau spectral method (Gottlieb et al., 1984). This entails transforming problem (1)–(12) to one on the interval $-1 \le x \le 1$ by letting $x \to \frac{2}{L}x - 1$. Assuming there will be no confusion, we keep the original variables x, w_i, ϕ_i, $i = 1, 2$, and the resulting system is

$$\omega^2 w_1(x) = \frac{2\widehat{k}}{L}\phi_1'(x) - \frac{4\widehat{k}}{L^2}w_1''(x) + C_1[w_2(x) - w_1(x)] \tag{47}$$

$$\omega^2 \phi_1(x) = -\frac{4E}{\sigma L^2}\phi_1''(x) + \widetilde{k}\phi_1(x) - \frac{2\widetilde{k}}{L}w_1'(x) \tag{48}$$

$$\omega^2 w_2(x) = \frac{2\widehat{k}}{L}\phi_2'(x) - \frac{4\widehat{k}}{L^2}w_2''(x) - C_2[w_2(x) - w_1(x)] \tag{49}$$

$$\omega^2 \phi_2(x) = -\frac{4E}{\sigma L^2}\phi_2''(x) + \widehat{k}\phi_2(x) - \frac{2\widehat{k}}{L}w_2'(x), \qquad -1 \le x \le 1, \tag{50}$$

$$\frac{2}{L}w_1'(-1) - \phi_1(-1) = 0 \tag{51}$$

$$\phi_1'(-1) = 0 \tag{52}$$

$$\frac{2}{L}w_2'(1) - \phi_2(-1) = 0 \tag{53}$$

$$\phi_2'(-1) = 0 \tag{54}$$

$$\widetilde{k}\phi_1(1) - \frac{2\widehat{k}}{L}w_1'(1) = -i\omega\alpha_1 w_1(1) \tag{55}$$

$$\frac{\partial E}{\sigma L}\phi_1'(1) = i\omega\beta_1\phi_1(1) \tag{56}$$

$$\widetilde{k}\phi_2(1) - \frac{2\widetilde{k}}{L}w_2'(1) = -i\omega\alpha_2 w_2(1) \tag{57}$$

$$\frac{\partial E}{\sigma L}\phi_2'(1) = i\omega\beta_2\phi_2(1). \tag{58}$$

We let

$$w_1(x) = \sum_{n=0}^{N} a_n P_n(x), \qquad \phi_1(x) = \sum_{n=0}^{N} b_n P_n(x),$$
$$w_2(x) = \sum_{n=0}^{N} c_n P_n(x), \qquad \phi_2(x) = \sum_{n=0}^{N} d_n P_n(x),$$

where P_n is the Legendre polynomial of degree n.
We then compare coefficients of x^n, for $n = 0, 1, \ldots, N-2$, in each of the equations resulting from (47)–(50) and, including the 8 equations resulting from boundary conditions (51)–(58),

the result is a system of $4N+4$ equations in the $4N+4$ unknowns a_n, b_n, c_n, d_n, $n = 0, 1, \ldots, N$, and the parameter ω. We may rewrite the system in the form

$$(\omega^2 A + \omega B + C)(a_0, \ldots, a_N, b_0, \ldots, b_N, c_0, \ldots, c_N, d_0, \ldots, d_N)^T = 0, \tag{59}$$

where A, B and C are $(4N+4) \times (4N+4)$ matrices. Then, the vibration spectrum consists of those numbers $-i\omega$, where ω is a latent value of (59), i.e., where ω satisfies

$$\det(\omega^2 A + \omega B + C) = 0. \tag{60}$$

It is easy to show that ω satisfies (60) if and only if ω is an eigenvalue of the $(8N+8) \times (8N+8)$ matrix

$$\begin{bmatrix} -A^{-1}B & -A^{-1}C \\ I & 0 \end{bmatrix},$$

where I is the $(4N+4) \times (4N+4)$ identity matrix and 0 the $(4N+4) \times (4N+4)$ 0-matrix. In practice, A is often singular—indeed, that is the case here. We remedy the situation by letting

$$\omega = \frac{\zeta - 1}{\zeta + 1},$$

yielding the equation

$$\det(\zeta^2 X + \zeta Y + Z),$$

where X, Y, Z, of course, are $(4N+4) \times (4N+4)$ matrices X is nonsingular, so we may proceed by finding the eigenvalues of

$$\begin{bmatrix} -X^{-1}Y & -X^{-1}Z \\ I & 0 \end{bmatrix}$$

and transforming back.

5. Comparison of numerical and asymptotic results

Assumptions (29) imply that $k_1 = k_2$ and $A_1/I_1 = A_2/I_2$. While, as mentioned above, this means that we are not looking at a double-walled tube, these assumptions have the advantage of allowing us better to see the effect that the damping parameters and Van der Waals force have on the imaginary parts—i.e., the actual "frequency" parts—of the eigenfrequencies, as we shall see below.

Form our physical and geometrical parameters, we choose the carbon nanotube data given in (Wang et al., 2006). Thus, we have E =1 TPa, G =.4 TPa, A =2.3090706 nm^2, I =.459649366 nm^4 and ρ =2.3 g/cm^3, and with a Van der Waals constant of C =.06943 TPa. Further, from our previous work, we have seen that, as the value of the slenderness ratio L/d increases, one must go further out along the spectrum in order to find agreement with the asymptotic results. Thus we choose L =2.5 nm, resulting in L/d =2.85714286.

The dimensionless parameters then become

$$\gamma_1 = .03185$$
$$\gamma_2 = .0652925$$
$$C' = .5729492131.$$

For the damping constants, there is nothing in the literature to guide our choices. However, we can see that, if each $\alpha_i'' < 1$ and each $\beta_i'' < 1$ in (43)–(46), the asymptotic behavior of the imaginary parts of the eigenfrequencies will behave as though both right ends are free; similarly, if the arguments in the logs all are negative, the behavior will be as if both right ends are clamped. (Of course, there are many more possibilities; however, "clamped" and "free" are the most common types, so, due to space limitations, we restrict ourselves to these two cases. Also, we mention that the critical cases $\alpha'' = 1$ and $\beta'' = 1$ are studied in (Coleman & Schaffer, preprint), for the single Timoshenko beam.) Further, our choices are guided by the wish to see clearly the separation of the spectrum into branches.

To study the case where the right ends are free-like, we choose our dimensionless damping parameters to be

$$\alpha_1' = .2, \quad \beta_1' = .01, \quad \alpha_2' = .1, \quad \beta_2' = .001. \tag{61}$$

For clamped-like, we choose:

$$\alpha_1' = .3, \quad \beta_1' = .013, \quad \alpha_2' = 2, \quad \beta_2' = .02. \tag{62}$$

For all of our numerical examples, we have performed computations at $N = 180$, 200 and 220 Legendre polynomials, and we see that all results have converged to at least 10 decimal places.

1) For our first example, we consider the case with damping parameters given by (61) and with no Van der Waals force. This will give us a baseline for later examples, and will allow us to see how the spectrum separates into four branches. The results can be seen in Tables 1A and 1B, where we actually separate the frequencies into their four branches. First, however, we must note that the branching is an asymptotic phenomenon, thus one needs to go out along the spectrum before it can be seen. As mentioned earlier, for larger values of L/d, one must go very far out before one sees the branching starting to occur. Here, we begin to see the branching and agreement with the asymptotic results pretty clearly after about the 4th or 5th eigenfrequency of each branch. For the first few, however, it may not even make sense to assign them to a branch; thus, while we do so by making our best guess, we mark them with $*$ to denote the fact that this assignment is problematic.

Table 1A, then, lists the first 40 eigenfrequencies, and the 50th, 60th, 70th, 80th, 90th and 100th eigenfrequencies, of each α-branch. The final column lists the asymptotic approximations for the imaginary parts, and the line at the bottom gives the asymptotic approximations for the real parts. Table 1B does the same, but for the β-branches.

As mentioned, in both tables the frequencies seem clearly to have split into branches, based on the real parts, well before the 10th frequency. By the 100th frequency in each branch, we have at least a three-decimal place match between the numerical and asymptotic real parts, and a four-decimal place match between the numerical and asymptotic imaginary parts.

One item of note: we see that the first frequency of the α-branch predicted by the asymptotic results does not appear. As we shall see, it appears that this frequency may have been "damped out" by the boundary damping.

2) For Example 2, we use the damping parameters given in (62), and Tables 2A and 2B are analogous to Tables 1A and 1B, respectively. Here, it is not clear how to deal with the first few entries in each table. However, they separate into branches very quickly. In Table 2A we see that, by the 100th frequency, we have at least a three-decimal place match between the numerical and asymptotic real parts, and a three-decimal- place match between the numerical and asymptotic imaginary parts. In Table 2B, by the 100th frequency we see a four-decimal place match between the numerical and asymptotic frequencies. Meanwhile, for

the β_2 branch, the numerical and asymptotic real parts match to three decimal places. For the β_1 branch, the match is not as good (two decimal places), though they still clearly seem to be converging.
For the remaining examples we introduce the Van der Waals force. Specifically, we wish to see what happens to the spectrum as the Van der Waals constant increases from 0 to about twice the value of the physically realistic value of $C' = .5729492131$. Thus, we consider what happens for the values

$$C' = 0, \quad .25, \quad .5, \quad .75 \quad \text{and} \quad 1.$$

3) For Examples 3 and 4, we look at two cases without boundary damping. Example 3 considers the case where the right ends are free, that is, for which

$$\alpha_1' = \beta_1' = \alpha_2' = \beta_2' = 0;$$

while Example 4 considers the right ends to be clamped, i.e.,

$$\alpha_1' = \beta_1' = \alpha_2' = \beta_2' = \infty.$$

We note that, in Examples 3 and 4, all numerical real parts are of absolute value $< 1.0E - 10$. The results for Example 3 can be found in Tables 3A and 3B. In Table 3A, we list the imaginary parts of the first 40 frequencies. The first column represents the double α- and β-branches, identical for $C' = 0$. Introducing $C' > 0$ leads to the splitting of these pairs. What is striking is that, for each pair of frequencies, one decreases as the value of C' increases, while the other is unaffected. (Indeed, it turns out that each of the even-numbered frequencies is unchanged to 13 decimal places!) Secondly, as we go out along the spectrum, the first member of each pair is less affected by the Van der Waals force, so that, when we get to the 39th–40th pair, they agree to three decimal places. (We look more closely at this phenomenon in Table 3B.)
Further, in comparing these results with those of Example 1, we see that the first predicted frequencies, missing in Table 1A, do appear here. Thus, as mentioned, it appears that the first pair was damped out via the boundary damping in Example 1, and that only one of these seems to be damped out by the inclusion of the Van der Waals force. Further, by comparing the first column of Table 3A with the results of Example 1, it is clear that the damping also affects the imaginary or "frequency" parts of the eigenfrequencies.
In Table 3B, we list the 49th–50th, 99th–100th, 149th–150th, 199th–200th, 249th–250th, 299th–300th, 349th–350th and 399th–400th eigenfrequencies, both numerical and asymptotic, for the case $C' = 1$ (i.e., corresponding to the last column in Table 3A). We see still closer agreement between the entries in each pair, and very close agreement with the asymptotics, as well. (Note that we list the branch for each eigenfrequency.) (Of course, the numbering here is very different from the numbering in Examples 1 and 2; e.g., the 40th entry in Table 3A corresponds to the 12th entry in Table 1A.)
4) The results of Example 4 are given in Tables 4A and 4B, in the same format as Tables 3A and 3B, respectively. In Table 4A, we see that the matching between the members of each pair is quite similar to that occurring in Table 3A. And again here, we see in Table 4B still closer agreement in each pair, and with the asymptotic results.
5) Example 5 is combination of Examples 1 and 3, and Example 6 is a combination of Examples 2 and 4. Example 5 looks at the damped system with the free-like parameters in (61), for the Van der Waals constant with values $C' = 0$, .5 and 1. The results are given in Tables 5A and 5B. In Table 5A, we proceed as in Table 3A, by listing the first 40 eigenfrequencies, although here we consider only the three values of C'. We see here that, for each pair, both

imaginary parts are affected by the Van der Waals force. However, we still see the closer matching of each pair as we go out along the spectrum. Meanwhile the real parts (damping rates) also are affected by the Van der Waals force, although there does not seem to be a noticeable pattern in that, in some cases it increases, while for others it decreases; in particular, there seems to be no branch-related pattern. Table 5B, then, is analogous to Table 3B, again using only the Van der Waals constant $C' = 1$. For the imaginary parts, the results are quite similar to those given in Table 3B. Meanwhile, the effect of the van der Waals on the real parts is diminished, as well, with the exception of the β_2-branch. However, this must be due to the fact that the β_2 damping rates are an order of magnitude smaller than the other damping rates.

6) In Table 6A, we proceed as in Table 4A, by listing the first 40 eigenfrequencies, but again only considering the three values of C'. We see again that, for each pair, both imaginary parts are affected by the Van der Waals force. Again we see the closer matching of each pair as we go out along the spectrum. Indeed, the last few pairs match more closely than the undamped pairs in Table 4A. The real parts behave quite the same as in Table 5A. Table 6B, then, is analogous to Table 4B, once more using only the Van der Waals constant $C' = 1$. Again, the imaginary parts behave quite similarly to those in Table 4B, and the real parts behave quite similarly to those in Table 5B.

In closing, we should mention that, although the results in (Shubov & Rojas-Arenaza, 2010b) show that the system is nonconservative, we have been unable to find any unstable eigenfrequencies in our numerical investigations.

	Numerical				Asymptotic (Im)
	α_1 Branch		α_2 Branch		
	Re	Im	Re	Im	
1.	—	—	—	—	6.14735
2.*	−2.746	9.44918	−.6783	9.93037	18.4421
3.*	−3.529	21.4099	−.9628	21.7742	30.7368
4.*	−3.658	39.8147	−1.490	38.6929	43.0315
5.	−3.823	53.2242	−.9151	51.9313	55.3262
6.	−4.613	64.3926	−.7899	65.1048	67.6209
7.	−4.754	77.6284	−.8924	78.0511	79.9156
8.	−4.696	90.6127	−1.224	90.7904	92.2103
9.	−4.357	103.890	−1.951	102.998	104.505
10.	−4.743	114.106	−1.357	114.409	116.800
11.	−4.902	127.122	−.7845	127.016	129.094
12.	−4.907	139.799	−.5884	139.671	141.389
13.	−4.690	152.112	−.5443	152.252	153.684
14.	−4.920	164.680	−.5754	164.776	165.979
15.	−4.899	177.203	−.6898	177.241	178.273
16.	−4.712	189.886	−.8915	189.528	190.568
17.	−4.831	201.386	−.8153	201.610	202.863
18.	−4.929	214.000	−.6139	213.968	215.157
19.	−4.932	226.449	−.5353	226.399	227.452
20.	−4.867	238.754	−.5199	238.814	239.747
21.	−4.934	251.173	−.5397	251.213	252.042
22.	−4.919	263.582	−.6054	263.584	264.336
23.	−4.715	276.142	−.7003	275.851	276.631

24.	−4.903	287.988	−.6383	288.060	288.926
25.	−4.937	300.421	−.5490	300.399	301.220
26.	−4.933	312.795	−.5165	312.766	313.515
27.	−4.926	325.094	−.5131	325.126	325.810
28.	−4.937	337.458	−.5304	337.478	338.104
29.	−4.923	349.829	−.5784	349.809	350.399
30.	−4.439	361.815	−.6217	362.065	362.694
31.	−4.929	374.314	−.5671	374.329	374.989
32.	−4.939	386.676	−.5232	386.661	387.283
33.	−4.929	399.021	−.5095	399.000	399.578
34.	−4.937	411.318	−.5110	411.335	411.873
35.	−4.937	423.655	−.5277	423.665	424.167
36.	−4.916	436.013	−.5653	435.973	436.462
37.	−4.870	448.131	−.5756	448.231	448.757
38.	−4.937	460.525	−.5344	460.523	461.052
39.	−4.940	472.857	−.5122	472.846	473.347
40.	−4.914	485.173	−.5068	485.171	485.641
50.	−4.791	608.231	−.5448	608.213	608.588
60.	−4.929	731.223	−.5045	731.223	731.535
70.	−4.869	854.207	−.5240	854.214	854.482
80.	−4.935	977.194	−.5038	977.195	977.429
90.	−4.940	1100.15	−.5155	1100.17	1100.38
100.	−4.938	1223.14	−.5034	1223.14	1223.32
Asym. Re:	−4.941		−.5027		

Table 1A. Numerical eigenfrequencies 1–40, 50, 60, 70, 80, 90 and 100 for the α_1 and α_2 branches from Example 1. The asymptotic imaginary parts are given in the last column, while the asymptotic real parts appear at the bottom.

	Numerical				Asymptotic (Im)
	β_1 Branch		β_2 Branch		
	Re	Im	Re	Im	
1.*	−2.335	27.3749	−1.321	26.9029	8.80167
2.*	−3.537	35.5415	−3.172	36.5570	26.4050
3.*	−5.139	51.3999	−4.007	50.2773	44.0084
4.*	−6.082	67.0480	−3.538	67.8770	61.6117
5.	−6.339	83.3545	−3.632	83.7187	79.2150
6.	−5.939	100.464	−4.061	99.7040	96.8184
7.	−6.716	118.544	−3.738	118.957	114.422
8.	−7.386	135.540	−3.642	135.511	132.025
9.	−7.623	152.566	−3.874	152.736	149.628
10.	−7.641	169.729	−3.682	169.794	167.232
11.	−7.510	187.131	−3.879	186.797	184.835
12.	−7.625	204.784	−3.775	205.036	202.438
13.	−7.843	222.194	−3.695	222.184	220.042
14.	−7.919	239.557	−3.762	239.624	237.645
15.	−7.900	256.965	−3.713	256.973	255.248
16.	−7.830	274.497	−3.920	274.214	272.852
17.	−7.903	292.103	−3.738	292.187	290.455

18.	−7.995	309.592	−3.715	309.577	308.059
19.	−8.018	327.064	−3.725	327.096	325.662
20.	−7.990	344.566	−3.728	344.549	343.265
21.	−7.957	362.152	−4.213	362.406	360.869
22.	−8.015	379.737	−3.726	379.758	378.472
23.	−8.057	397.260	−3.730	397.244	396.075
24.	−8.060	414.783	−3.723	414.796	413.679
25.	−8.032	432.332	−3.743	432.293	431.282
26.	−8.027	449.937	−3.790	450.040	448.885
27.	−8.068	467.510	−3.726	467.512	466.489
28.	−8.087	485.056	−3.749	485.055	484.092
29.	−8.081	502.606	−3.727	502.609	501.695
30.	−8.058	520.184	−3.772	520.119	519.299
31.	−8.069	537.788	−3.740	537.822	536.902
32.	−8.095	555.359	−3.728	555.355	554.505
33.	−8.102	572.920	−3.732	572.931	572.109
34.	−8.091	590.488	−3.731	590.482	589.712
35.	−8.077	608.084	−3.875	608.067	607.315
36.	−8.095	625.681	−3.732	625.690	624.919
37.	−8.110	643.255	−3.732	643.248	642.522
38.	−8.110	660.826	−3.730	660.831	660.125
39.	−8.098	678.408	−3.738	678.391	677.729
40.	−8.094	696.011	−3.760	696.054	695.332
50.	−8.119	871.910	−3.733	871.914	871.365
60.	−8.130	1047.85	−3.732	1047.85	1047.40
70.	−8.134	1223.82	−3.735	1223.82	1223.43
80.	−8.135	1399.80	−3.733	1399.80	1399.47
90.	−8.138	1575.80	−3.734	1575.80	1575.50
100.	−8.141	1751.80	−3.734	1751.80	1751.53
Asym. Re:	−8.143		−3.734		

Table 1B. Numerical eigenfrequencies 1–40, 50, 60, 70, 80, 90 and 100 for the β_1 and β_2 branches from Example 1. The asymptotic imaginary parts are given in the last column, while the asymptotic real parts appear at the bottom.

	Numerical				Asymptotic (Im)
	α_1 Branch		α_2 Branch		
	Re	Im	Re	Im	
1.*					12.2947
2.*	−2.961	9.93687	−1.610	12.4325	24.5894
3.	−3.190	29.3701	−1.397	31.1896	36.8841
4.	−4.064	46.0071	−1.634	45.0854	49.1788
5.	−4.495	57.8442	−1.657	58.5989	61.4735
6.	−4.053	71.8202	−1.621	71.7962	73.7682
7.	−4.142	85.2854	−1.523	84.8430	86.0630
8.	−4.567	98.6461	−1.323	98.0245	98.3577
9.	−5.318	105.571	−1.169	106.236	110.652
10.	−4.540	119.808	−1.533	120.191	122.947
11.	−4.216	133.109	−1.633	133.237	135.242

12.	−4.218	146.000	−1.647	145.953	147.536
13.	−4.179	158.522	−1.639	158.542	159.831
14.	−4.174	171.218	−1.612	171.110	172.126
15.	−4.406	183.978	−1.517	183.787	184.421
16.	−5.446	194.130	−1.130	194.144	196.715
17.	−4.348	207.405	−1.571	207.533	209.010
18.	−4.164	220.088	−1.624	220.138	221.305
19.	−4.165	232.619	−1.631	232.603	233.599
20.	−4.143	245.025	−1.628	245.027	245.894
21.	−4.161	257.514	−1.613	257.457	258.189
22.	−4.348	270.059	−1.540	269.988	270.484
23.	−4.753	281.519	−1.352	281.352	282.778
24.	−4.211	294.071	−1.603	294.130	295.073
25.	−4.138	306.548	−1.623	306.566	307.368
26.	−4.151	318.951	−1.625	318.946	319.662
27.	−4.130	331.320	−1.623	331.313	331.957
28.	−4.159	343.734	−1.611	343.694	344.252
29.	−4.363	356.177	−1.518	356.192	356.547
30.	−4.346	367.985	−1.536	367.969	368.841
31.	−4.155	380.426	−1.614	380.456	381.136
32.	−4.129	392.820	−1.622	392.824	393.431
33.	−4.138	405.165	−1.622	405.168	405.725
34.	−4.128	417.522	−1.620	417.511	418.020
35.	−4.164	429.902	−1.607	429.873	430.315
36.	−4.414	442.219	−1.394	442.404	442.609
37.	−4.204	454.269	−1.595	454.287	454.904
38.	−4.133	466.654	−1.618	466.669	467.199
39.	−4.127	479.008	−1.621	479.006	479.494
40.	−4.127	491.332	−1.621	491.334	491.788
50.	−4.211	614.282	−1.579	614.263	614.735
60.	−4.122	737.376	−1.619	737.377	737.682
70.	−4.162	860.323	−1.600	860.315	860.630
80.	−4.120	983.347	−1.619	983.347	983.577
90.	−4.138	1007.97	−1.612	1007.96	1106.52
100.	−4.120	1130.91	−1.618	1130.91	1129.47
Asym. Re:	−4.118		−1.618		

Table 2A. Numerical eigenfrequencies 1–40, 50, 60, 70, 80, 90 and 100 for the α_1 and α_2 branches from Example 2. The asymptotic imaginary parts are given in the last column, while the asymptotic real parts appear at the bottom.

	Numerical				Asymptotic (Im)
	α_1 Branch		α_2 Branch		
	Re	Im	Re	Im	
0.*	−2.767	20.7386	−.3306	20.7810	
1.*	−3.365	32.4318	−.3818	31.1907	17.6033
2.*	−4.405	43.3261	−.4055	44.5802	35.2067
3.	−4.889	59.8085	−.4281	59.3359	52.8100
4.	−5.844	74.6045	−.5117	74.9216	70.4134

5.	−5.926	90.1511	−.7273	90.8426	88.0167
6.	−5.396	112.518	−.8981	112.008	105.620
7.	−6.281	127.780	−.5491	127.584	123.223
8.	−6.594	144.098	−.4656	144.153	140.827
9.	−6.736	161.038	−.4744	161.084	158.430
10.	−6.648	177.856	−.5675	178.041	176.033
11.	−5.663	197.373	−.9579	197.391	193.637
12.	−6.785	213.821	−.5208	213.750	211.240
13.	−6.945	230.896	−.4746	230.912	228.843
14.	−6.990	248.188	−.4806	248.215	246.447
15.	−6.852	265.397	−.5525	265.465	264.050
16.	−6.465	283.725	−.7417	283.906	281.653
17.	−7.012	300.977	−.4935	300.948	299.257
18.	−7.061	318.329	−.4777	318.336	316.860
19.	−7.077	335.745	−.4853	335.769	334.464
20.	−6.892	353.121	−.5783	353.106	352.067
21.	−6.916	371.147	−.5602	371.174	369.670
22.	−7.105	388.547	−.4836	388.536	387.274
23.	−7.118	406.017	−.4793	406.019	404.877
24.	−7.109	423.484	−.4901	423.506	422.480
25.	−6.866	441.016	−.7033	440.833	440.084
26.	−7.079	458.824	−.5031	458.814	457.687
27.	−7.144	476.297	−.4809	476.297	475.290
28.	−7.150	493.819	−.4809	493.822	492.894
29.	−7.114	511.317	−.4975	511.331	510.497
30.	−6.958	529.040	−.6926	529.212	528.100
31.	−7.142	546.621	−.4875	546.611	545.704
32.	−7.161	564.142	−.4806	564.143	563.307
33.	−7.164	581.683	−.4828	581.690	580.910
34.	−7.098	599.211	−.5157	599.200	598.514
35.	−7.092	616.952	−.5196	616.974	616.117
36.	−7.169	634.487	−.4829	634.483	633.720
37.	−7.173	652.039	−.4810	652.039	651.324
38.	−7.167	669.587	−.4853	669.595	668.927
39.	−7.070	687.169	−.5948	687.091	686.530
40.	−7.153	704.848	−.4913	704.845	704.134
50.	−7.188	880.714	−.4823	880.711	880.167
60.	−7.195	1056.65	−.4817	1056.65	1056.20
70.	−7.199	1232.61	−.4820	1232.61	1232.23
80.	−7.197	1408.59	−.4836	1408.59	1408.27
90.	−7.206	1584.59	−.4821	1584.59	1584.30
100.	−7.176	1760.61	−.4824	1760.61	1760.33
Asym. Re:	−7.208		−.4821		

Table 2B. Numerical eigenfrequencies 1–40, 50, 60, 70, 80, 90 and 100 for the β_1 and β_2 branches from Example 2. The asymptotic imaginary parts are given in the last column, while the asymptotic real parts appear at the bottom.

	$C' = 0$	$C' = .25$	$C' = .5$	$C' = .75$	$C' = 1$
1.	2.9458212164	1.2833048444	—	—	—
2.	2.9458212164	2.9458212164	2.9458212164	2.9458212164	2.9458212164
3.	10.678276269	10.429210089	10.173172662	9.9095407887	9.6376145423
4.	10.678276269	10.678276269	10.678276269	10.678276269	10.678276269
5.	22.186791607	22.071993648	21.956728997	21.840975799	21.724712242
6.	22.186791607	22.186791607	22.186791607	22.186791607	22.186791607
7.	26.977657335	26.925021146	26.872366881	26.819700315	26.767023640
8.	26.977657335	26.977657335	26.977657335	26.977657335	26.977657335
9.	36.385895938	36.330795486	36.275730248	36.220689467	36.165662881
10.	36.385895938	36.385895938	36.385895938	36.385895938	36.385895938
11.	39.346020018	39.290455669	39.234922527	39.179434389	39.123994694
12.	39.346020018	39.346020018	39.346020018	39.34602002	39.346020018
13.	50.846627673	50.805226033	50.763519267	50.721507452	50.679174702
14.	50.846627673	50.846627673	50.846627673	50.846627673	50.846627673
15.	52.832231307	52.792215617	52.752514490	52.713137027	52.674092535
16.	52.832231307	52.832231307	52.832231307	52.832231307	52.832231307
17.	64.810103855	64.762969581	64.715722238	64.668361902	64.620894071
18.	64.810103855	64.810103855	64.810103855	64.810103855	64.810103855
19.	67.511260081	67.495035827	67.478904495	67.462874126	67.446934409
20.	67.511260081	67.511260081	67.511260081	67.511260081	67.511260081
21.	77.945061900	77.902776945	77.860470284	77.818146754	77.775801859
22.	77.945061900	77.945061900	77.945061900	77.945061900	77.945061900
23.	83.358682455	83.347923221	83.337147524	83.326356066	83.315549557
24.	83.358682455	83.358682455	83.358682455	83.358682455	83.358682455
25.	90.953565995	90.918343817	90.883145591	90.847963440	90.812804258
26.	90.953565995	90.953565995	90.953565995	90.953565995	90.953565995
27.	99.219305787	99.204551012	99.189697002	99.174754327	99.159714381
28.	99.219305787	99.219305787	99.219305787	99.219305787	99.219305787
29.	104.36226852	104.33801023	104.31384569	104.28976275	104.26577156
30.	104.36226852	104.36226852	104.36226852	104.36226852	104.36226852
31.	113.79274626	113.76791681	113.74302537	113.71805740	113.69303441
32.	113.79274626	113.79274626	113.79274626	113.79274626	113.79274626
33.	119.25906418	119.24966905	119.24033598	119.23105702	119.22184083
34.	119.25906418	119.25906418	119.25906418	119.25906418	119.25906418
35.	126.98609223	126.95906982	126.93201897	126.90494972	126.87787207
36.	126.98609223	126.98609223	126.98609223	126.98609223	126.98609223
37.	135.64225489	135.63853685	135.63483364	135.63113319	135.62744782
38.	135.64225489	135.64225490	135.64225489	135.64225489	135.64225489
39.	139.71595073	139.69029336	139.66462947	139.63895904	139.61328206
40.	139.71595073	139.71595073	139.71595073	139.71595073	139.71595073

Table 3A. The first 40 imaginary parts of the numerical eigenfrequencies from Example 3, computed for five different values of the Van der Waals constant C'. The "real-life" value of the constant is approximately .57.

	Numerical	Asymptotic
49.	177.211	178.283 (α-branch)

50.	177.293	178.283 ″
99.	361.308	360.869 (β-branch)
100.	361.331	360.869 ″
149.	537.847	536.902 (β-branch)
150.	537.848	536.902 ″
199.	718.895	719.240 (α-branch)
200.	718.916	719.240 ″
249.	903.393	903.661 (α-branch)
250.	903.410	903.661 ″
299.	1083.03	1082.61 (β-branch)
300.	1083.03	1082.61 ″
349.	1260.06	1260.21 (α-branch)
350.	1260.07	1260.21 ″
399.	1444.46	1444.62 (α-branch)
400.	1444.47	1444.62 ″

Table 3B. Numerical and asymptotic eigenfrequencies (imaginary parts) 49, 50, 99, 100, 149, 150, 199, 200, 249, 250, 299, 300, 349, 350, 399, 400 from Example 3, computed for the Van der Waals constant $C' = 1$.

	$C' = 0$	$C' = .25$	$C' = .5$	$C' = .75$	$C' = 1$
1.	12.98454240	12.82401972	12.66021095	12.49299083	12.32222077
2.	12.98454240	12.98454240	12.98454240	12.98454240	12.98454240
3.	20.80444376	20.73055727	20.65705225	20.58390602	20.51109394
4.	20.80444376	20.80444376	20.80444376	20.80444376	20.80444376
5.	31.18843099	31.12463266	31.06111752	30.99788409	30.93493102
6.	31.18843099	31.18843099	31.18843099	31.18843099	31.18843099
7.	31.24700816	31.18715530	31.12710108	31.06685140	31.00640685
8.	31.24700816	31.24700816	31.24700816	31.24700816	31.24700816
9.	44.57678921	44.53928646	44.50196213	44.46481864	44.42785126
10.	44.57678921	44.57678921	44.57678921	44.57678921	44.57678921
11.	45.09876440	45.04148608	44.98405651	44.92647256	44.86873484
12.	45.09876440	45.09876440	45.09876440	45.09876440	45.09876440
13.	58.59976143	58.54891895	58.49801214	58.44703446	58.39599137
14.	58.59976143	58.59976143	58.59976143	58.59976143	58.59976143
15.	59.33988894	59.31872578	59.29763244	59.27660934	59.25566107
16.	59.33988894	59.33988894	59.33988894	59.33988894	59.33988894
17.	71.76457338	71.72043968	71.67628715	71.63210155	71.58790511
18.	71.76457338	71.76457338	71.76457338	71.76457338	71.76457338
19.	74.95903748	74.94532704	74.93161035	74.91790464	74.90420214

20.	74.95903748	74.95903748	74.95903748	74.95903748	74.95903748
21.	84.79872934	84.76134601	84.72397393	84.68660688	84.64925063
22.	84.79872934	84.79872934	84.79872934	84.79872934	84.79872934
23.	90.88275651	90.86960300	90.85639777	90.84314155	90.82983509
24.	90.88275651	90.88275651	90.88275651	90.88275651	90.88275651
25.	97.98924692	97.96005606	97.93091660	97.90181859	97.87277054
26.	97.98924692	97.98924692	97.98924692	97.98924692	97.98924692
27.	106.2587082	106.2388530	106.2189144	106.1988926	106.1787763
28.	106.2587082	106.2587082	106.2587082	106.2587082	106.2587082
29.	111.9946283	111.9779469	111.9613540	111.9448287	111.9283915
30.	111.9946283	111.9946283	111.9946283	111.9946283	111.9946283
31.	120.2222931	120.1964306	120.1705341	120.1445952	120.1186307
32.	120.2222931	120.2222931	120.2222930	120.2222931	120.2222931
33.	127.5643741	127.5578845	127.5514182	127.5449753	127.5385763
34.	127.5643741	127.5643741	127.5643741	127.5643741	127.5643741
35.	133.2540877	133.2279431	133.2017948	133.1756314	133.1494527
36.	133.2540877	133.2540877	133.2540878	133.2540877	133.2540877
37.	144.1489244	144.1458534	144.1427760	144.1397215	144.1366607
38.	144.1489244	144.1489244	144.1489244	144.1489244	144.1489244
39.	145.9551025	145.9304056	145.9056787	145.8809675	145.8562415
40.	145.9551025	145.9551025	145.9551025	145.9551025	145.9551025

Table 4A. The first 40 imaginary parts of the numerical eigenfrequencies from Example 4, computed for five different values of the Van der Waals constant C'.

	Numerical	Asymptotic
49.	183.705	184.421 (α-branch)
50.	183.779	184.421 ″
99.	367.917	368.841 (α-branch)
100.	367.955	368.841 ″
149.	546.609	545.704 (β-branch)
150.	546.609	545.704 ″
199.	725.047	725.388 (α-branch)
200.	725.068	725.388 ″
249.	909.548	909.808 (α-branch)
250.	909.565	909.808 ″
299.	1091.80	1091.41 (β-branch)
300.	1091.80	1091.41 ″
349.	1267.85	1267.44 (β-branch)
350.	1267.85	1267.44 ″
399.	1450.61	1450.78 (α-branch)
400.	1450.62	1450.78 ″

Table 4B. Numerical and asymptotic eigenfrequencies (imaginary parts) 49, 50, 99, 100, 149, 150, 199, 200, 249, 250, 299, 300, 349, 350, 399, 400 from Example 4, computed for the Van der Waals constant $C' = 1$.

	$C' = 0$		$C' = .5$		$C' = 1$	
	Re	Im	Re	Im	Re	Im
1.	—	—	—	—	—	—
2.	—	—	—	—	—	—
3.	−2.746	9.449183995	−2.877	9.172044078	−2.972	8.827341448
4.	−.6783	9.930366988	−.7344	9.678929479	−.8576	9.477841762
5.	−3.529	21.40990132	−3.575	21.29275588	−3.611	21.16999982
6.	−.9628	21.77418316	−.9720	21.65493676	−.9945	21.54041229
7.	−1.321	26.90292372	−1.312	26.85129816	−1.308	26.79542808
8.	−2.335	27.37492665	−2.342	27.32751386	−2.343	27.28372611
9.	−3.537	35.54153378	−3.556	35.47898352	−3.569	35.40700136
10.	−3.172	36.55704093	−3.177	36.50955538	−3.190	36.47367372
11.	−1.490	38.69290303	−1.496	38.63128423	−1.504	38.56575342
12.	−3.658	39.81469654	−3.664	39.76185775	−3.665	39.71104768
13.	−4.007	50.27733227	−4.028	50.23454838	−4.048	50.18747340
14.	−5.139	51.39985683	−5.143	51.37684915	−5.148	51.35549893
15.	−.9151	51.93127198	−.9182	51.87409462	−.9225	51.81686142
16.	−3.823	53.22422671	−3.821	53.18663028	−3.816	53.15176710
17.	−4.613	64.39259632	−4.626	64.34564444	−4.637	64.29753890
18.	−.7899	65.10483274	−.7935	65.05533361	−.7986	65.00630011
19.	−6.082	67.04799021	−6.082	67.03545255	−6.081	67.02281832
20.	−3.538	67.87701409	−3.539	67.86205923	−3.539	67.84780896
21.	−4.754	77.62836514	−4.762	77.58540148	−4.768	77.54197597
22.	−.8924	78.05109828	−.8968	78.00762380	−.9026	77.96449011
23.	−6.339	83.35453188	−6.335	83.34816855	−6.331	83.34180146
24.	−3.632	83.71862800	−3.635	83.70997652	−3.638	83.70136960
25.	−4.696	90.61268633	−4.700	90.57580895	−4.703	90.53866701
26.	−1.224	90.79035136	−1.230	90.75096706	−1.237	90.71182474
27.	−4.061	99.70402490	−4.068	99.69160776	−4.076	99.67839224
28.	−5.939	100.4640803	−5.931	100.4692419	−5.924	100.4751321
29.	−1.951	102.9983756	−1.960	102.9543524	−1.970	102.9099689
30.	−4.352	103.8895026	−4.350	103.8631919	−4.346	103.8372742
31.	−4.743	114.1061665	−4.749	114.0804654	−4.754	114.0546217
32.	−1.357	114.4090098	−1.352	114.3757397	−1.348	114.3424705
33.	−6.716	118.5438854	−6.722	118.5429195	−6.727	118.5418301
34.	−3.738	118.9568732	−3.736	118.9487280	−3.735	118.9408092
35.	−.7845	127.0161580	−.7832	126.9880193	−.7825	126.9598517
36.	−4.902	127.1222585	−4.906	127.0951053	−4.909	127.0679252
37.	−3.642	135.5114464	−3.642	135.5080511	−3.642	135.5046704
38.	−7.386	135.5399041	−7.388	135.5375232	−7.390	135.5351432
39.	−.5884	139.6706311	−.5884	139.6447863	−.5888	139.6189351
40.	−4.907	139.7988314	−4.910	139.7733338	−4.912	139.7478086

Table 5A. The first 40 numerical eigenfrequencies from Example 5, computed for three different values of the Van der Waals constant C.

	Numerical Re	Numerical Im	Asymptotic Re	Asymptotic Im
49.	−4.902	177.162	−4.941	178.283 (α_1-branch)
50.	−.6921	177.198	−.5027	178.283 (α_2-branch)
99.	−7.957	362.152	−8.143	360.869 (β_2-branch)
100.	−4.195	362.404	−3.734	360.869 (β_1-branch)
149.	−8.069	537.788	−8.143	536.902 (β_2-branch)
150.	−3.740	537.822	−3.734	536.902 (β_1-branch)
199.	−.5069	718.904	−.5027	719.240 (α_2-branch)
200.	−4.941	718.909	−4.941	719.240 (α_1-branch)
249.	−4.940	903.399	−4.941	903.661 (α_1-branch)
250.	−.5046	903.403	−.5027	903.661 (α_2-branch)
299.	−3.734	1083.03	−3.734	1082.61 (β_1-branch)
300.	−8.127	1083.03	−8.143	1082.61 (β_2-branch)
349.	−.5123	1260.02	−.5027	1260.21 (α_2-branch)
350.	−4.923	1260.04	−4.941	1260.21 (α_1-branch)
399.	−.5053	1444.46	−.5027	1444.62 (α_2-branch)
400.	−4.940	1444.46	−4.941	1444.62 (α_1-branch)

Table 5B. Numerical and asymptotic eigenfrequencies (imaginary parts) 49, 50, 99, 100, 149, 150, 199, 200, 249, 250, 299, 300, 349, 350, 399, 400 from Example 5, computed for the Van der Waals constant $C' = 1$.

	$C' = 0$ Re	$C' = 0$ Im	$C' = .5$ Re	$C' = .5$ Im	$C' = 1$ Re	$C' = 1$ Im
1.	−2.961	9.936871385	−3.079	9.795166383	−3.169	9.644727421
2.	−1.610	12.43254005	−1.618	12.28811944	−1.632	12.14607344
3.	−2.767	20.73861326	−2.794	20.64458863	−2.815	20.55053147
4.	−.3306	20.78104522	−.3395	20.70597402	−0.355	20.63293559
5.	−3.190	29.37005728	−3.187	29.32574131	−3.182	29.28091887
6.	−1.397	31.18963235	−.3840	31.12726000	−.3882	31.06474018
7.	−.3818	31.19073440	−1.392	31.12875704	−1.390	31.06625299
8.	−3.365	32.43182622	−3.369	32.36004659	−3.369	32.28961412
9.	−4.405	43.32612319	−4.402	43.28601387	−4.398	43.24625757
10.	−.4055	44.58018737	−.4065	44.54246627	−.4083	44.50537030
11.	−1.634	45.08538379	−1.632	45.02792865	−1.634	44.96962880
12.	−4.064	46.00707085	−4.068	45.95274391	−4.070	45.89830745
13.	−4.495	57.84423832	−4.479	57.81269810	−4.461	57.78159556
14.	−1.657	58.59889870	−1.656	58.54816779	−1.659	58.49709714
15.	−.4281	59.33578065	−.4286	59.31422388	−.4295	59.29277982
16.	−4.889	59.80848155	−4.905	59.76734039	−4.920	59.72601742
17.	−1.621	71.79615374	−1.620	71.75209563	−1.621	71.70774465

18.	−4.053	71.82019141	−4.045	71.78210831	−4.037	71.74432634
19.	−5.844	74.60448514	−5.849	74.58483733	−5.854	74.56510945
20.	−.5117	74.92157699	−.5133	74.90763370	−.5152	74.89373280
21.	−1.523	84.84297209	−1.522	84.80549984	−1.522	84.76785224
22.	−4.142	85.28536486	−4.141	85.25105512	−4.140	85.21691580
23.	−5.926	90.15112979	−5.923	90.13610573	−5.920	90.12104814
24.	−.7273	90.84264675	−.7301	90.82960542	−.7331	90.81651834
25.	−1.323	98.02449900	−1.320	97.99508254	−1.319	97.96567545
26.	−4.567	98.64607511	−4.570	98.61744170	−4.573	98.58888833
27.	−5.318	105.5709742	−5.311	105.5523351	−5.304	105.5336172
28.	−1.169	106.2355904	−1.173	106.2156779	−1.177	106.1956428
29.	−.8981	112.0084405	−.8948	111.9918049	−.8917	111.9752688
30.	−5.396	112.5178851	−5.403	112.4994593	−5.409	112.4810878
31.	−4.540	119.8083113	−4.535	119.7838877	−4.530	119.7594125
32.	−1.533	120.1912992	−1.535	120.1654629	−1.536	120.1395677
33.	−.5491	127.5842376	−.5480	127.5777146	−.5471	127.5712440
34.	−6.281	127.7796866	−6.285	127.7714673	−6.288	127.7632923
35.	−4.216	133.1088121	−4.214	133.0838601	−4.211	133.0588793
36.	−1.633	133.2370084	−1.634	133.2109568	−1.635	133.1848771
37.	−6.594	144.0977330	−6.594	144.0939736	−6.594	144.0902605
38.	−.4656	144.1532932	−.4655	144.1501251	−.4654	144.1469825
39.	−1.647	145.9530993	−1.647	145.9284497	−1.648	145.9037766
40.	−4.218	145.9995218	−4.218	145.9750728	−4.217	145.9505817

Table 6A. The first 40 numerical eigenfrequencies from Example 6, computed for three different values of the Van der Waals constant C'.

	Numerical		Asymptotic	
	Re	Im	Re	Im
49.	−1.516	183.750	−1.618	184.421 (α_2-branch)
50.	−4.408	183.941	−4.118	184.421 (α_1-branch)
99.	−1.538	367.949	−1.618	368.841 (α_2-branch)
100.	−4.344	367.965	−4.118	368.841 (α_1-branch)
149.	−.4874	546.610	−.4821	545.704 (β_2-branch)
150.	−7.142	546.620	−7.208	545.704 (β_1-branch)
199.	−1.619	725.057	−1.618	725.388 (α_2-branch)
200.	−4.122	725.058	−4.118	725.388 (α_1-branch)
249.	−1.618	909.557	−1.618	909.808 (α_2-branch)
250.	−4.121	909.559	−4.118	909.808 (α_1-branch)
299.	−.4987	1091.80	−.4821	1091.41 (β_2-branch)
300.	−7.168	1091.81	−7.208	1091.41 (β_1-branch)
349.	−7.173	1267.83	−7.208	1267.44 (β_1-branch)
350.	−.5013	1267.84	−.4821	1267.44 (β_2-branch)

399.	−4.120	1450.61	−4.118	1450.78 (α_2-branch)
400.	−1.618	1450.61	−1.618	1450.78 (α_1-branch)

Table 6B. Numerical and asymptotic eigenfrequencies (imaginary parts) 49, 50, 99, 100, 149, 150, 199, 200, 249, 250, 299, 300, 349, 350, 399, 400 from Example 6, computed for the Van der Waals constant $C' = 1$.

6. References

Coleman, M.P. & Schaffer, L. (2010). Asymptotic analysis of the vibration spectrum of coupled Timoshenko beams with a dissipative joint, *Eur. J. Mech. A Solids*, Vol. 29, No. 4, 629-636.

Coleman, M.P. & Schaffer, L. The single Timoshenko beam with general boundary damping, an asymptotic and numerical study, preprint.

Gibson, R.F.; Ayorinde, E.O. & Wen, Y.-F. (2007). Vibrations of carbon nanotubes and their composites: A review, *Comp. Sci. Tech.*, Vol. 67, 1-27.

Gottlieb, D.; Hussaini, M.Y. & Orszag, S.A. (1984). Theory and applications of spectral methods, *Spectral methods for partial differential equations* , pp. 1-54, Hampton, VA, 1982, SIAM, Philadelphia, PA.

Jakobson, B.I.; Brabec, C.J. & Berhold, J. (1996). Nanomechanics of carbon nanotubes: Instabilities beyond linear response, *Phys. Rev. Lett.*, Vol. 76, No. 14, 2511-2514.

Jamieson, V. (2000). Carbon nanotubes roll on, *Phys. World*, Vol. 13, No. 6, 29-30.

Mahan, G.D. (2002). Oscillations of a thin hollow cylinder: Carbon nanotubes, *Phys. Rev. B*, Vol. 65, No. 23, 235402.1-235402.7.

Pantano, A.; Boyce, M.C. & Parks, D.M. (2003). Nonlinear structural mechanics based modeling of carbon nanotube deformation, *Phys. Rev. Lett.*, Vol. 91, No. 14, 145504.1-145504.4.

Pantano, A.; Boyce, M.C. & Parks, D.M. (2004). Mechanics of deformation of single and multi-wall carbon nanotubes, *J. Mech. Phys. Solids*, Vol. 52, No. 4, 789-821.

Qian, D.; Wagner, G.J.; Liu, W.K.; Yu, M.-F. & Ruoff, R.S. (2002). Mechanics of carbon nanotubes, *Appl. Mech. Rev.*, Vol. 55, No. 6, 495-533.

Ru, C.Q. (2000). Effect of Van der Waals forces on axial buckling of a double-walled carbon nanotube, *J. Appl. Phys.*, Vol. 87, 1712-1715.

Ru, C.Q. (2001). Degraded axial buckling strain of multiwalled carbon nanotubes due to interlayer slips, *J. Appl. Phys.*, Vol. 89, No. 6, 3426-3433.

Shubov, M.A. & Rojas-Arenaza, M. (2010a). Vibrational frequency distribution for nonconservative model of double-walled carbon nanotube, *Appl. Math. Comput.*, Vol. 217, No. 3, 1246-1252.

Shubov, M.A. & Rojas-Arenaza, M. (2010b). Mathematical analysis of carbon nanotube model, *J. Comput. Appl. Math.*, Vol. 234, No. 6, 1631-1636.

Shubov, M.A. & Rojas-Arenaza, M. (2010c). Asymptotic distribution of eigenvalues of dynamics generator governing vibrations of double-walled carbon nanotube model, *Asymptotic Anal.*, Vol. 68, No. 1–2, 89-124.

Traill-Nash, R.W. & Collar, A.R. (1953). The effects of shear flexibility and rotatory inertia on the bending vibrations of beams, *Quart. J. Mech. Appl. Math.*, Vol. 6, 186-222.

Wang, C.M.; Tan, V.B.C. & Zhang, Y.Y. (2006). Timoshenko beam model for vibration analysis of multi-walled carbon nanotubes, *J. Sound Vibrations*, Vol. 294, 1060-1072.

Wang, C.Y.; Ru, C.Q. & Mioduchowski, A. (2004). Applicability and limitations of simplified elastic shell equations for carbon nanotubes, *J. Appl. Mech.*, Vol. 71, 622-631.
Wang, C.Y.; Ru, C.Q. & Mioduchowski, A. (2005). Free vibrations of multiwall carbon nanotubes, *J. Appl. Phys.*, Vol. 97, 114323.1-114323.10.
Wang, Q. (2005). Wave propagation in carbon nanotubes via nonlocal continuum mechanics, *J. Appl. Phys.*, Vol. 98, 124301.
Xu, K.Y.; Guo, X.N. & Ru, C.Q. (2006). Vibration of a double-walled carbon nanotube aroused by nonlinear intertube Van der Waals forces, *J. Appl. Phys.*, Vol. 99, 064303.1-064303.7.
Yoon, J.; Ru, C.Q. & Mioduchowski, A. (2003). Vibration of an embedded multiwall carbon nanotube, *Comp. Sci. Tech.*, Vol. 63, 1533-1542.

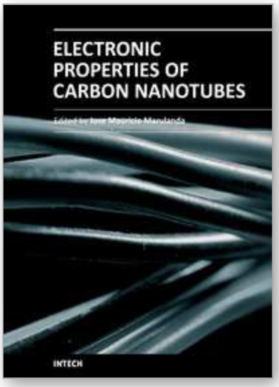

Electronic Properties of Carbon Nanotubes

Edited by Prof. Jose Mauricio Marulanda

ISBN 978-953-307-499-3
Hard cover, 680 pages
Publisher InTech
Published online 27, July, 2011
Published in print edition July, 2011

Carbon nanotubes (CNTs), discovered in 1991, have been a subject of intensive research for a wide range of applications. These one-dimensional (1D) graphene sheets rolled into a tubular form have been the target of many researchers around the world. This book concentrates on the semiconductor physics of carbon nanotubes, it brings unique insight into the phenomena encountered in the electronic structure when operating with carbon nanotubes. This book also presents to reader useful information on the fabrication and applications of these outstanding materials. The main objective of this book is to give in-depth understanding of the physics and electronic structure of carbon nanotubes. Readers of this book should have a strong background on physical electronics and semiconductor device physics. This book first discusses fabrication techniques followed by an analysis on the physical properties of carbon nanotubes, including density of states and electronic structures. Ultimately, the book pursues a significant amount of work in the industry applications of carbon nanotubes.